PROC. OF JSCE
No. 292, December 1979

BEHAVIOR OF CONCRETE PLATES JOINED TO COLUMNS

By Jun YAMAZAKI and Neil M. HAWKINS***

1. INTRODUCTION

(1) The Nature of the Problem

If a flat slab is to resist lateral forces, moments must be transferred between slab and column as would be apparent from consideration of the situation shown in Fig. 1. Further, even where lateral forces are resisted by shear walls or other framing systems, some moment transfer must occur at edge, corner and first interior columns. Transfer can also occur at other interior columns due to uneven live loads on adjacent spans, uneven lengths for adjacent spans, and uneven changes in column lengths.

Besides the flat slab buildings, the similar problem of the stress transfer could occur in a portion of plates, true plates or very flat shell elements, rigidly connected to other framing structural members; for example, in bridge decks, pierdecks, containers, caissons or ship hulls.

Tests on flat slab structures[1] have shown that under gravity loads almost complete redistribution of moments in the slab can be achieved prior to collapse provided a premature punching failure can be avoided at the slab column connection. The possibility of the punching failure is enhanced when moment transfer occurs. In several tests on slab systems[1] the failures have been initiated at connections where moment transfer was observed or was possible, and these failures have occurred at strengths less than those predicted by the ACI Code 318-77[2]. The lack of understanding of the factors controlling the strength, stiffness and ductility of slab to column connections is a bottleneck restraining the wider use of flat plate construction, especially for framing systems designed to resist lateral forces. In order to provide the required understanding there is a need for additional test data, and a method of analysis that takes account of the known inelastic effects. That method must be more than another empirical procedure.

(2) Background

The present state of knowledge on the shear strength and behavior of reinforced and prestressed concrete flat slabs has been summarized by ACI-ASCE Committee 426[1] and will not be repeated here. In this section, a review is made of some of the main characteristics of the problem identified in earlier studies and of some design considerations.

a) Shear Transfer

Previous investigations[1)~3)] have cleary shown that shear failures of slab column connections are a combined shear and flexure problem. The studies by Kinnunen and Nylander[4),5)] have demonstrated that the circumferential stiffness of the slab has a marked effect on the strength of a slab column connection. In conformity with that concept their tests showed that the strength and ductility of slab-column connections increased as the circumferential stiffness for the slab increased, either as a result of an increase in the amount of reinforcement or a change in the type of reinforcement to one with a higher circumferential stiffness. Kinnunen and Nylander's results have also shown that the development of an inclined crack does not lead to immediate failure. They observed inclined cracks at between 45 and 75 percent of the failure loads. Further, while the strength

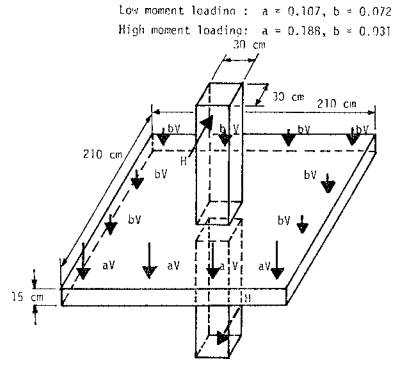

Fig. 1 Slab-column specimen.

* Associate Professor, Tokyo Metropolitan University
** Professor, University of Washington

of specimens with preformed inclined cracks was 50 to 60 percent of the strength of identical solid specimens there was no appreciable reduction in stiffness because of the preformed cracks. The results suggest that at loads greater than 50 percent of the ultimate loads inclined cracking may only indirectly affect the stiffness of a solid slab. That indirect effect probably permits a beneficial redistribution of stresses. The difficulty of making an idealized model to predict the observed behavior, even for a loading case with polar symmetry, is also clearly demonstrated by Kinnunen and Nylander's investigations.

b) Moment and Shear Transfer

Method of ACI Code 318-77[2]. The method of analysis suggested in the commentary to ACI Code 318-77, Section 11.12.2 is a modification of a procedure developed originally by Di Statio and Van Buren[6] in 1960. As shown in Fig. 2 it is presumed that the shear stresses on the critical perimeter vary linearly with distance from the centroidal axis of that perimeter. Maximum shear stresses are then given by the formula

$$v_{AB}=\frac{V_u}{A_c}+\frac{\gamma_v M_u c_{AB}}{J_c}$$

or

$$v_{CD}=\frac{V_u}{A_c}-\frac{\gamma_v M_u c_{CD}}{J_c}$$

in which

$$A_c=2\,d(x+y)$$

$$J_c=\frac{y^3 d}{6}+\frac{y d^3}{6}+\frac{dxy^2}{2}$$

v_{AB}, v_{CD}=the nominal shear stresses on face AB and CD

$\gamma_v M_u$=fraction of the total moment transferred by shear

d=effective depth of slab

x, y=horizontal dimensions of the critical section

V_u=applied shear

Various investigations have recommended values for αd which determines the dimension x and y in Fig. 2, ranging from 0 to 3 times slab thickness.

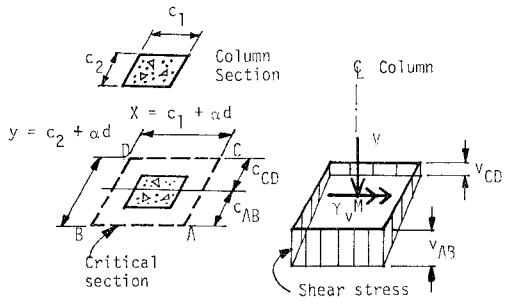

Fig. 2 Assumed distribution of shear stress per ACI code procedure.

ACI Code 318-77 requires the use of α equal to unity. One approach to the evaluation of $\gamma_v M_u$ has been to take $\gamma_v M_u$ as that portion of the moment not transferred by flexure across faces AB and CD. That was the procedure originally used by Di Statio and Van Buren. The other approach has been to assume γ_v to be a constant evaluated empirically from test data. That was the procedure originally proposed by Moe[7], and the same procedure is used for ACI Code.

When moment is transferred between a slab and a column torsions must develop at the side faces of the column. Hanson and Hanson's results[8] indicate that the torsional strength of those faces is significantly higher than the torsional strength of the isolated beams with similar cross sections subjected to pure torsions.

The method for predicting the strength of slab-column connections contained in ACI Code 318-77 is based on hypothesis in which one parameter and the maximum nominal shear stress are determined empirically from test results. The ACI Code method appears to neither take proper account of the actual strengths of the different segments of the critical section, nor to realistically simulate the actual stress distribution on those segments.

Beam Analogy. Hawkins and Corley[9] proposed a model for which the slab sections framing into each column face are idealized as beam sections with a width $(c+d)$ or $(c+d/2)$ as appropriate, where c is the side length of the column and d is effective depth of slab. Each beam section is presumed capable of developing at the critical perimeter the ultimate bending moment, torque, shear, and combination of those quantities as independent beams. Redistribution of applied shear forces and moment is permitted between adjacent beams and failure is presumed to occur when ultimate capacities are developed for three adjacent beam sections.

2. FINITE ELEMENT ANALYSES OF SLAB-COLUMN CONNECTIONS

(1) Model

For prediction of the strength of a slab-column connection it is important to understand how forces applied to the slab are carried in the region immediately adjacent to the column, and to understand the mechanism by which those forces redistribute themselves around a connection as the stiffness of the slab changes. The proportions for the column and slab chosen for the analyses were idealization of those of the slab-column specimens reported in the Appendix. The proportions for those specimens are shown in Fig. 1. The behavior was examined

for the two loading cases which were referred as the high moment loading when moment to shear ratio, M/V was equal to 58 cm, and the low moment loading when this ratio was 13 cm. Method of application of these loads are indicated in Fig. 1 and the Appendix.

For reinforced concrete cracking of the concrete, debonding of the reinforcing bars, yielding of those bars and inelastic deformations of the concrete all place limitations on the effectiveness of a routine application of the finite element methods. The mesh layout selected for this study is shown in Fig. 3. The smallest element measured 7.6 cm square and was located adjacent to the column. The side dimension for that element was half the slab thickness, one quarter of the column side length and approximately 0.4 times the reinforcing bar spacing, so that as cracking, debonding, or yielding should occur, resultant local effects are likely to be confined to approximately the area of the element in which that effect is predicted. In later discussions, partial compensation is also made for the possible use of an inappropriate mesh size, by integrating or averaging force values for discrete segment of the vertical section surrounding a connection, before making comparisons.

The boundary for the slab was specified as fixed at the column perimeter. In reality that boundary deforms due to cracking of the concrete or yielding and debonding of the reinforcing bars. The discrepancy between the real and assumed boundary conditions at the column perimeter undoubtedly introduces errors into the computation of deformation. However, since the slab is supported by a single column and is externally statically determinate, the errors in computation of stresses under ultimate conditions are likely to be small provided the joint is able to develop the same strength as the slab in the adjacent region.

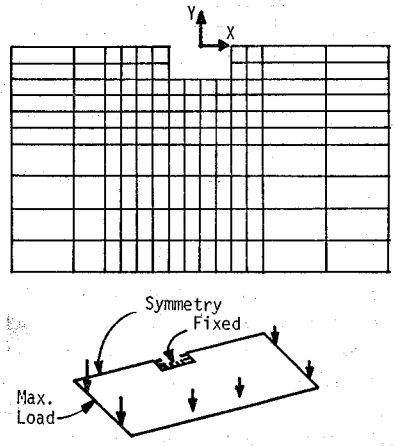

Fig. 3 Finite element idealization.

The effect of diagonal tension cracking on the stiffness of the elements and the distribution of stresses was not considered. Thus, information on stresses obtained from these analyses may not be indicative of the actual conditions in the slab at failure unless propagations of the diagonal tension cracks are restrained by adequate shear reinforcement.

(2) Plate Bending Finite Element Method

For this analysis the program used was a simplified version of that developed by Clough and Felippa[12]. Contrary to statements in the original reference, the program used for this study did not include the effects of shear distortion. For the elastic range of behavior the slab was assumed to be isotropic. For inelastic analysis the slab was treated as an orthotropic plate with the direction of the orthotropy coincident with the directions of the reinforcement, and with the stiffness in the orthogonal directions dependent on the yield conditions for that reinforcement.

An imaginary incremental modulus of elasticity was selected such that the flexural stiffness EI for the 15 cm thick plate was equal to the actual incremental stiffness calculated for the reinforced concrete section. A moment-curvature relationship was computed assuming a linear distribution of strain over the depth of the section and using the average effective depth to the reinforcing steel. The actual stress-strain curve was used for the reinforcing bars and assumed stress-strain curve for the concrete. The concrete curve consited of a second order parabola for the ascending branch of the curve and a straight line for the descending branch as proposed by Hognestad. Concrete was assumed capable of carrying a tensile stress equal to the modulus of rupture for calculation of section properties. A typical resultant moment-curvature relationship could be approximated by a bi-linear curve. Cracked section was assumed from the start of loading.

The resultant E value was 65 000 kg/cm^2 prior to yielding and 0.04 times that value subsequent to yielding for the solid 15 cm thick plate that had equivalent moment-curvature relationship.

(3) Yield Criterion

The standard plate bending program was extended into the inelastic range by assuming the stiffness of the elements to be linearly elastic for a small increment in load. The magnitude of load increment was determined so that it caused yielding in at least one new element when the major principal moment exceeded the yield strength of the element. A tolerance of 5 percent was used for computational convenience. The element stiffness based on the

stiffness in the directions of reinforcement at each stage was varied according to the magnitude of the major principal moments in the element. Thus, three cases for the element stiffness was possible, namely, those for elastic behavior, yielding of the reinforcement in one direction, and yielding of the reinforcement in both directions.

When a slab contained equal amounts of reinforcement in two orthogonal directions, yielding seldom occurs in the two directions simultaneously. Yielding in the less heavily stressed reinforcement was assumed to occur when the curvature in the direction of that reinforcement became equal to the curvature in the direction of the more heavily stressed reinforcement at the load stage for yielding of that reinforcement. Based on the work by Lenschow and Sozen[10] and Cardenas and Sozen[11] the following simplified procedure was used. First, the ratio R_{21} of the curvature in the direction of the more heavily stressed reinforcement to the curvature in the orthogonal direction was calculated for the condition of the first yielding. For a particular case where this ratio remained constant for all subsequent load stages, second yielding was assumed to have occurred when the curvature in the more heavily stressed reinforcement equaled R_{21} times the curvature in that direction at first yielding.

The rational basis for this criterion is apparent from an examination of the deformations of the reinforced concrete plate element shown in Fig. 4 as follows. The original undeformed position of the element is indicated by broken lines and the deformed position by solid lines. The relationship between the strains ε_{a1} at the level and in the direction of the bar, the nominal strains ε_n and ε_t, and the shearing strain γ_{nt} is given by

$$\varepsilon_{a1}=\varepsilon_n\cos^2\alpha+\varepsilon_t\sin^2\alpha+\gamma_{nt}\sin\alpha\cos\alpha\cdots(1)$$

In the direction of the orthogonal reinforcing bar, the strain ε_{a2} is

$$\varepsilon_{a2}=\varepsilon_n\sin^2\alpha+\varepsilon_t\cos^2\alpha-\gamma_{nt}\cos\alpha\sin\alpha\cdots(2)$$

When a slab element is reinforced in two orthogonal directions in such a manner that it has equal strengths in the two directions, the slab will be referred isotropically reinforced as was in reference 10) and 11).

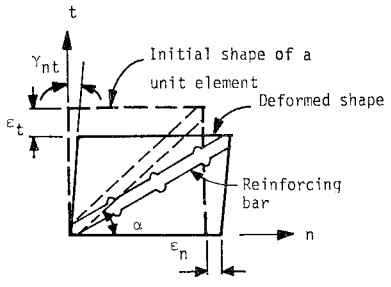

Fig. 4 Deformed shape of a unit element of a reinforced concrete plate.

For an isotropically reinforced concrete slab yield lines form perpendicular to the direction of the major principal moment so that γ_{nt} is zero on the yield line. For the condition that n and t are the principal directions and for Poisson's ratio equal to zero,

$$\frac{\varepsilon_t}{\varepsilon_n}=\frac{M_t}{M_n}\cdots(3)$$

where M_n and M_t are the major and minor principal moments. Thus,

$$R_{21}=\frac{\varepsilon_{a1}}{\varepsilon_{a2}}=\frac{M_n\cos^2\alpha+M_t\sin^2\alpha}{M_n\sin^2\alpha+M_t\cos^2\alpha}\cdots(4)$$

If the moment at first yielding is M_y and "1" is the direction of the most heavily stressed reinforcement then in subsequent load stages, the moment M_1, in the most heavily stressed reinforcement will increase because of the bi-linear moment curvature relationship. If that moment is given by

$$M_1=M_y+M_p\cdots(5)$$

then the curvature in the 1 direction can be obtained by dividing M_1 by the stiffness. Thus the criterion for second yielding is for the moment in the most heavily loaded direction to satisfy

$$\frac{M_y/C_y+M_p/C_p}{M_y/C_y}=\frac{\varepsilon_y+\varepsilon_p}{\varepsilon_y}=R_{21}\cdots(6)$$

where C_y is the stiffness at first yielding, and C_p is the incremental stiffness in the subsequent load stages, ε_p is the increase in strain in the subsequent load stages, and ε_y is the strain for first yielding.

For any small element contained within the slab of the slab-column specimen the proportions and the directions of the moments will change with load as yielding occurs in the surrounding elements. For simplicity and in order not to overestimate the stiffness of an element, the factor R_{21} was calculated for each load stages subsequent to first yielding and the calculated deformation compared with the value of R_{21} at first yielding and the current load stage. If the calculated deformation exceeded the smaller value of those two, yielding was assumed to have occurred in the sceond direction. For the inelastic range of behavior about sixteen load increments were used to compute the response between conditions for first yielding and those for general failure of the slab.

(4) Validity of Assumptions.

In order to examine the effects of neglecting shear distortions in the plate bending finite element methods and validity of calculating transverse shears by moment equilibrium, deflections and stresses computed by the plate bending method for the elastic range of behavior were compared with those computed by general theory of elasticity methods. The characteris-

tics of the three dimensional solid element developed by Wilson and the improvement in accuracy obtained with this element are described in reference 13). The elements in this method are based on isoparametric formulation. Three translational deflections, three normal stresses and three shear stresses were computed for the center and top face of each element. The plate was represented by one layer of prismatic elements with an identical horizontal discretization to the thin plate model.

After examination of bending and twisting moments major differences were found to occur in twisting moment for the elements surrounding the column corners. For those elements twisting moments computed by the elasticity method were maximum, while for plate method the same moments are small. This difference probably results from the manner in which deformations are idealized for thin plate theory. In thin plate theory the twisting moment is considered proportional to the distortion as expressed by the term $\partial^2 w/\partial x \partial y$ where w is the plate deflection. Thus, thin plate theory does not have a capability for representing shear distortions within the plain of the plate. Therefore, for the corner elements the twisting moments predicted by the elasticity method was used for computation of the principal moments for first load increment.

Comparison of transverse shear stresses on the perimeter located 15 cm (slab thickness) from the column shown in Fig. 5 revealed that although maximum difference is as much as 50 percent above the value computed by the elasticity method, when averages are compared for sections along each column face shown in Fig. 5, the variation predicted by the two methods was small. The proportions of the total shear entering the front, side and back faces of the column as designated in Fig. 5 were about the same according to the two methods. The total shears predicted by the two methods were about 93 and 91 percent of the applied shear with better agreement being recorded for the elasticity method.

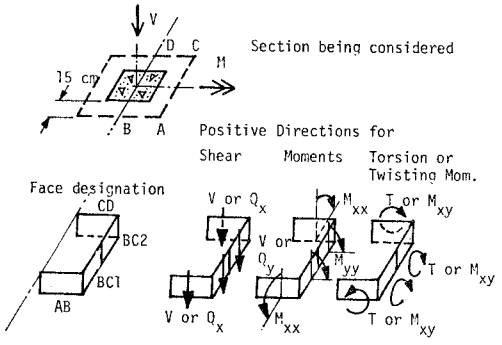

Fig. 5 Selected location for evaluation of stress resultants.

Shear and moment stress resultants were evaluated by integration of stresses on appropriate critical areas on the same perimeter, and the contribution of each resultant to the transfer of moment to column was examined. The sign convention for positive values and the locations of the sections *AB*, *BC*, and *CD* are shown in Fig. 5. The torsion on the side face *BC* consisted of that caused by horizontal shear stress, or twisting moment, and that caused by transverse shear. Good agreement of the results by the two methods was obtained as shown below.

Table 1

Percent of applied moment resisted by	Low Moment Loading		High Moment Loading	
	Theory of Elasticity	Theory of Thin plates	Theory of Elasticity	Theory of Thin plates
Bending, Face *AB* and *CD*	24	23	34	32
Shear, Face *AB* and *CD*	36	35	31	29
Torsion (Twisting moment)	11	12	10	11
Torsion (Transverse shear)	19	21	17	19
Total	90	91	92	91

From the comparisons it can be concluded that although there are a number of instances where results predicted by the elasticity and thin plate methods differ, overall trends are sufficiently similar to justify the use of the simpler plate bending methods for analyses in the inelastic range. Difference in deflection was less than 10 percent.

Deformation characteristics of reinforced concrete slab studied in reference 10 and 11 implies that, if the reinforced concrete slab was idealized as a homogeneous isotropic plate having an elastic modulus E in the direction of orthogonal reinforcement, the shear modulus G should be approximately equal to $E/4$ rather than $E/2$ as would be the case for a homogeneous elastic material, if Poisson's effect is neglected. It was found that use of G equal to $E/2$ as in this study would result in overestimate of stiffness, if a predominant moment acts in a direction much deviating from the direction of reinforcing bars. The average of such overestimate in all elements was evaluated to be about 10 percent for low moment loading and 20 percent for high moment loading.

(5) Predicted Inelastic Behavior.

The yield lines predicted by the analysis and their order of development are shown in Fig. 6. In this figure also shown are the principal moments at the ultimate. Significant changes in the directions of the major principal moment with load was found to occur for the segment of the slab in front of the column. In that region radial moments dominated

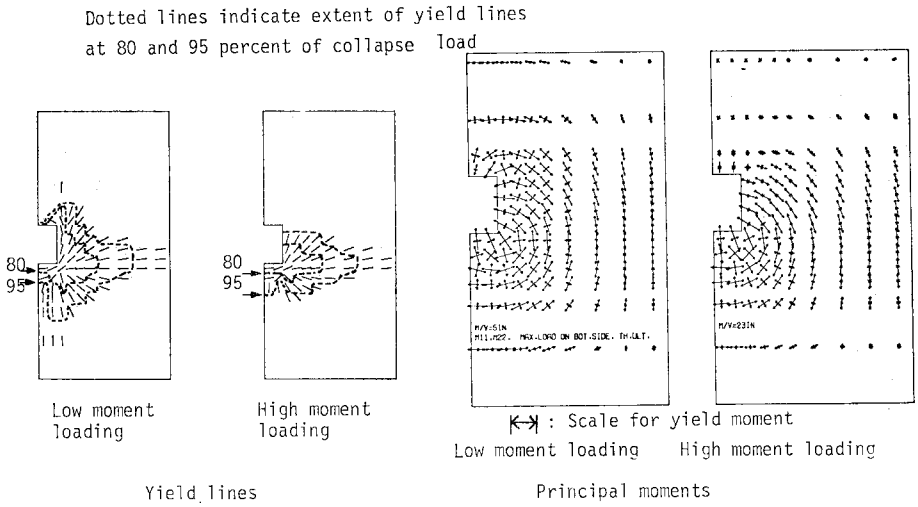

Fig. 6 Predicted directions of yield lines and principal moments.

at first yielding but tangential moments dominated at collapse. For both loading cases yielding was predicted in the both directions of reinforcement for only three intersections closest to the front corner of the column. The collapse mechanism for both loading cases can be called a wide beam mechanism with a hinge line all the way across the width of the slab. The load causing this mechanism can be found approximately by simple statics, and this load will be referred as theoretical flexurel strength. The inclination of the yield lines from the line perpendicular to the direction of the applied unbalanced moment implies a capacity less than that given by simple statics. However, that effect is more than compensated by strain hardening effect for the reinforcement. The actual failure mode and ultimate strength may differ from what have been described above based on the pure flexural yield criterion of slab element, because sections of the slab may fail in reality due to torsion, transverse shear or combination of those and flexure.

An isometric diagram for the distribution of moments M_{xx} and M_{yy} for high moment loading case is shown in Fig. 8. The definition of stresses is shown in Fig. 5. The direction of moment M_{xx} coincides with the direction of the applied unbalanced moment. The first diagram corresponds to the elastic limit, the second to the theoretical flexural strength, and the last diagram is the difference between the first two and represents the amount of redistribution of stresses. From the first diagram for M_{xx} a high concentration of the stress is observed in the front face AB of the column. From the second and the last diagrams it is apparent that in subsequent load stages more moment is redistributed toward the edges of the slab due to progressive development of yield lines as shown in Fig. 6. Also shown in this diagram is that this moment causes tension on the bottom of the slab in the back side of the column CD. The diagram for M_{yy} shows another marked effect of redistribution of moment in transverse direction and pronounced intensity in front half of the side column face BC 1. A similar diagram in Fig. 9 shows the distribution of transverse shear Q_y. A large amount of redistribution is seen to occur in the front half of the side column face BC 1. This behavior was to be expected from the manner of redistribution of the moments described above. A high concentration of the shear stress is observed even at the theoretical flexural strength.

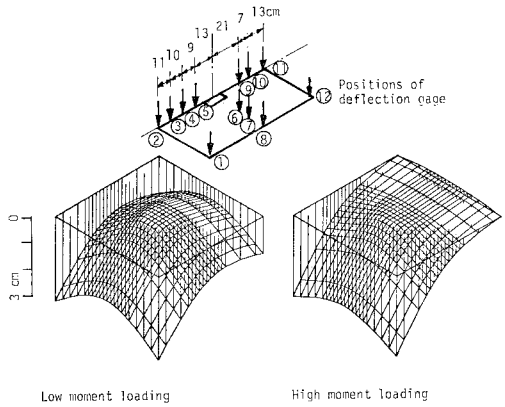

Fig. 7 Predicted deflections of slab.

(6) Stress Resultants on the Critical Sections.

Shown in Figs. 10 and 11 are stress resultants for the two loading cases for the critical section segments

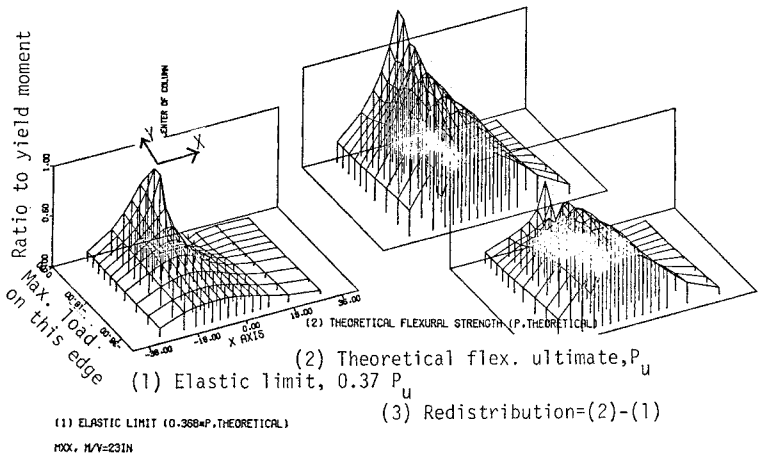

Fig. 8 (a) Distribution of moment M_{xx} for high moment loading.

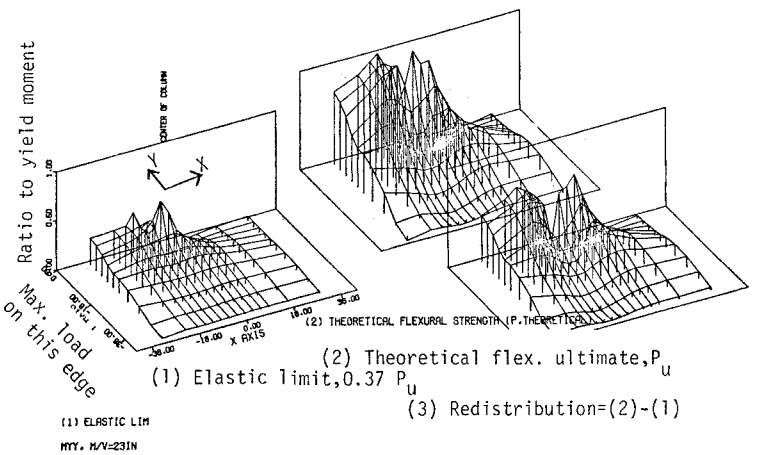

Fig. 8 (b) Distribution of moment M_{yy} for high moment loading.

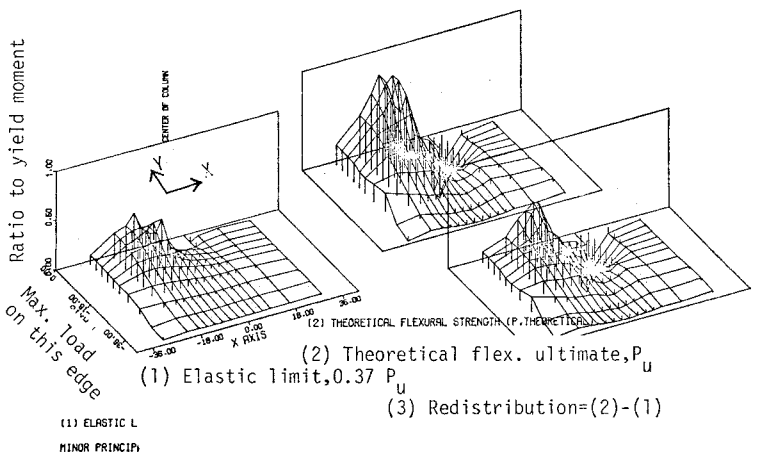

Fig. 8 (c) Distribution of minor principal moment for high moment loading.

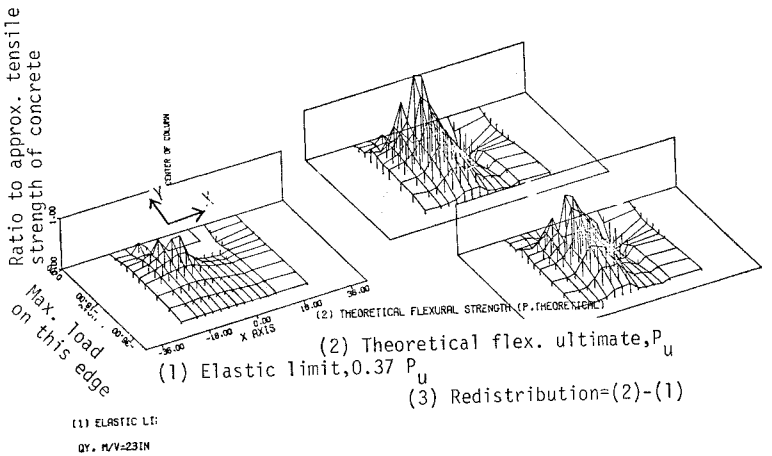

Fig. 9 Distribution of shear stress Q_y for high moment loading.

shown in Fig. 5. The section considered is located 15 cm (slab thickness) from the column perimeter. This location was the closest distance from the column where shear stresses could be evaluated with satisfactory accuracy, and within the variation of the critical location proposed by various investigations. It is likely that the same shear force will be carried across any geometrically similar section located closer to the column than the section shown in Fig. 5 and therefore probably no corrections to the shear force values in those diagrams need be considered for comparison with ACI Code requirements or for evaluation of shear at column faces. The resultants are considered positive when acting in the sense shown in Fig. 5. The torsional moments shown in Fig. 10 and 11 are the sum of the torsional effects caused by twisting moments (contribution of horizontal shear) and vertical shears.

a) High Moment Loading

From the results in Fig. 10 it is apparent that with increasing load there is a continuous redistribution between the various faces of the proportions of the total shear and moment transferred to the column. The decrease in the rate at which shear is attracted to the face *AB* and the increase for the face *BC*1, following the initiation of moment redistribution, can be attributed to the softening of the elements adjacent to face *AB* with yielding. However, once yielding also initiates for the elements adjacent to face *BC*1 that trend is reversed. Since the stiffness for the two faces are then about the same, the rate at which shears develop returns to about the rate for elastic behavior. Once yielding begins at the front face *AB* it is apparent that additional external moment is equilibrated by increase of the shears on faces *AB*, *BC*1 and *CD*, increase of the torsion on faces *BC*1 and *BC*2 and increase in the negative moment for face *CD*. On faces *BC*2 and *CD* the shears act upwards.

If limiting values of shear, moment and torsion exist separately for design purposes, it is obvious that the primary considerations must be the combination of shear and torsional effects for the face *BC*1 and the provision of adequate moment capacity for face *CD* given a certain moment capacity for face *AB*. In contrast, the ACI Code requirements are addressed primarily to shear

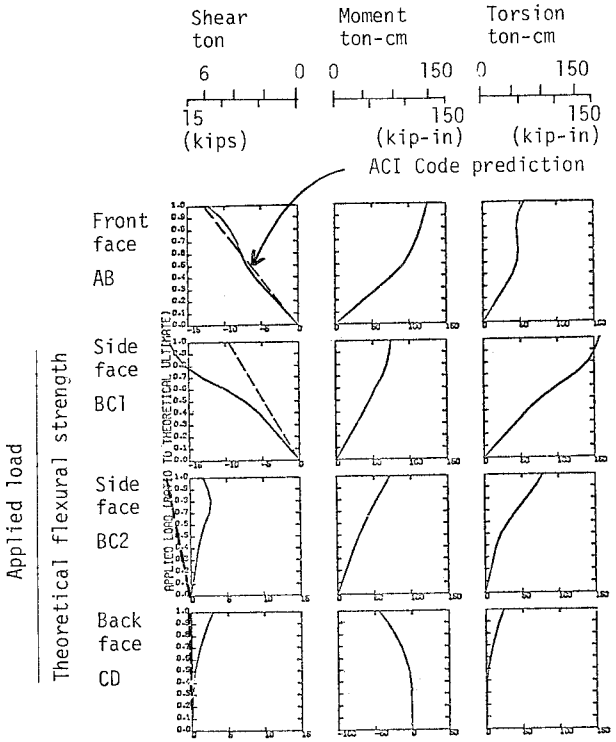

Fig. 10 Force distributions for high moment loading.

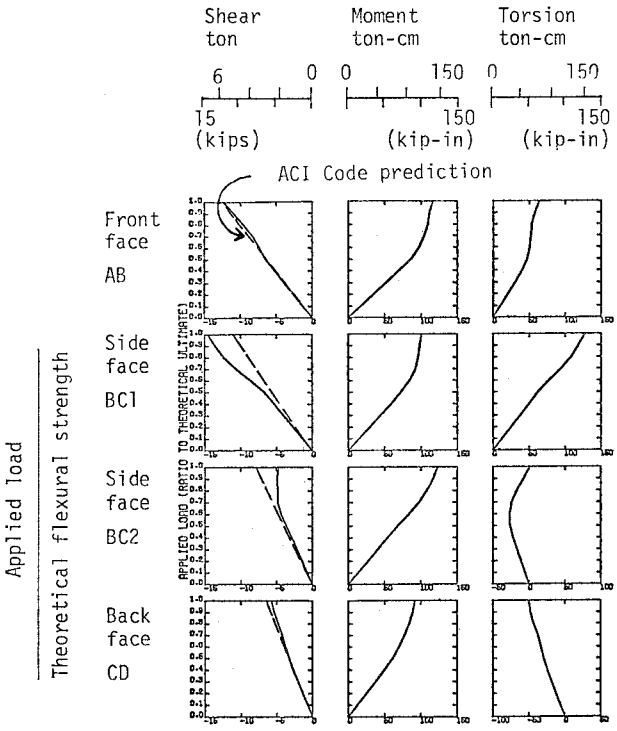

Fig. 11 Force distributions for low moment loading.

and moment capacities for the face *AB*. Further, it is apparent that it would be dangerous to design a connection subjected to a high moment loading on the basis of the elastic response predicted by a finite element analysis.

b) Low Moment Loading.

The results shown in Fig. 11 indicate that for higher loads the bending moment on face *BC*1 increases at a slower rate, that on *BC*2 develops at almost a constant rate until about 80 percent of the collapse load, and that on *CD* develops at a much slower rate. The rate which the torsional moment develops on face *BC*1 is little affected by first yielding. For face *BC*2, however, the torsional moment, which is opposite in sense to that on face *BC*1 at lower loads, reverses and for increasing loads increases so that at failure the torsional moment on face *BC*2 is in the same direction as that on *BC*1. Yielding has little overall effect on the rate at which shears develop on faces *AB* and *CD*. Yielding does result in the shears on face *BC*1 increasing at a faster rate and those on face *BC*2 increasing at a slower rate with increasing load than for elastic behavior.

From these results it is apparent that yielding initiates first at the face *AB*. The resultant softening requires that most of the additional moment transferred to the column for higher loads be resisted through the development of torsions and shears on the side faces at rates greater than those predicted for elastic behavior. From Fig. 10 it is apparent that the primary design considerations must be combination of shear, torsion and moment effects for face *BC*1 and the shear for face *AB*.

c) Comparison with the Shear Criterion of ACI Code.

In Figs. 10 and 11 the shear stress resultants for each of the four faces predicted by the ACI 318-77 provisions for moment transfer are indicated by broken lines. In Fig. 10 the shear predicted by the procedure in the ACI Code is negative for face *BC* 2 while that predicted by thin plate theory is positive. For face *CD* the shear predicted by the ACI Code is zero.

For both loading cases there is good agreement between the shear assigned to the face *AB* by ACI Code and that predicted by thin plate theory. For low moment loading the agreement for the other faces is also good for elastic behavior but poorer for inelastic behavior. While the total shear assigned to the face *BC* by both the ACI Code procedure and the thin plate method is similar, the distribution of stresses along that face according to the two methods differs radically. For high moment loading the agreement between the two methods for faces other than *AB* is poor, even for elastic behavior. According to the thin plate results the positive shears on faces *CD* and *BC*2 increases the total shear force to be resisted by faces *AB* and *BC*1. The Code predicts no such effect until a higher *M*/*V* ratio for the connection.

The results for the shear on face *AB* for high moment loading suggest that concentration of the reinforcement through that face may not be beneficial unless shear reinforcement is increased proportionately. Because the load for first yielding is increased, the shear on that face must increment at the elastic rate to a greater percentage of the ultimate capacity before any beneficial reduction in that rate with yielding is realized.

3. COMPARISON OF MEASURED AND PREDICTED RESULTS

(1) Test Specimen.

The test program was reported in the Appendix. For each loading condition results of one test specimen were referred for comparison. Each specimen was designated by three numerals indicating the percentage of flexural reinforcement, a character *E* indicating the test series, a character *L* or *H* indicating low or high moment loading and finally another set of three numerals indicating percentage of shear reinforcement in a 30 cm wide section. Thus the two specimen were identified as 0.96 EL 0.33 and 0.96 EH 0.33. Arrangement of reinforcement is shown in Fig. 16.

(2) Crack Patterns.

The direction of the potential cracks predicted by the analyses are shown in Fig. 12. Cracks were assumed to occur where a principal moment exceeded the cracking moment of the section. For the high moment loading the broken lines paralleling face *CD* indicate that cracking on the bottom rather than the top side of the slab is predicted. Shown in Fig. 13 is a reproduction of the crack pattern from the photographs of the specimens after the completion of the tests on those specimens. The crack patterns shown in Fig. 12 are in good agree-

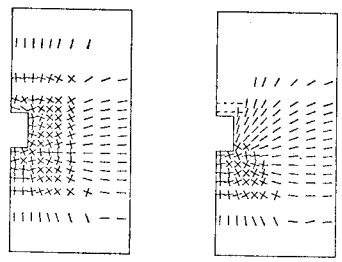

Fig. 12 Predicted directions and extent of cracking.

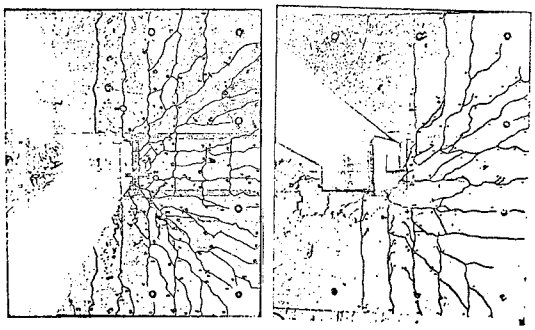

Fig. 13 Observed cracking.

ment with the measured patterns both as to the directions of cracking and the extent of craking. Cracks paralleling face *CD* and on the bottom side of the slab were observed in the test on specimens subjected to high moment loading. The occurrence of those cracks is one confirmation that the actual behavior closely paralleled that predicted by thin plate theory.

(3) Deflections and Deformations.

Changes in deflection with load are plotted in Figs. 14 and 15 for 5 points (Gage numbers D 1, 2, 3, 4, 5) on the front half of the slab, 3 points (Gage numbers D 6, 7, 8) on the side half of the slab and 4 points (Gage number D 9, 10, 11, 12) on the back half of the slab. The gage locations and predicted deformed shape of the slab are shown in Fig. 7. Deflections were measured to the nearest 0.25 mm. The deflections plotted in Figs. 14 and 15 are displacements relative to the column. Thus, the settlement and the rotation of the bottom column was subtracted from the measured deflection to obtain those values. Measured load-deflection relationships are shown on the right half and the same relationship predicted by plate bending analysis are shown on the left. The calculated and measured load-deflection curve show obvious similarities in their overall profile. However, the measured deflections for a given load are considerably greater than the calculated deflections. The measured deflections at about 70 percent of theoretical flexural strength was almost equal to final value for the calculated deflection.

For low moment loadings the measured deflections were downward at all gage points. For high moment loading both the calculated and measured deflections for the back half of the slab showed upward displacements close to collapse. The measured upward displacements increased markedly immediately prior to collapse, reaching values several times greater than the calculated displacements. In the ana-

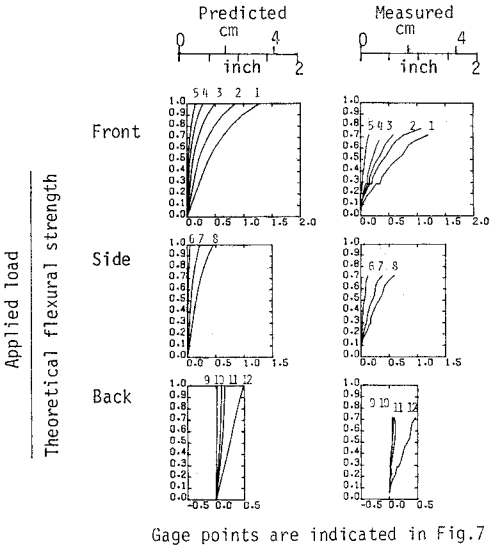

Fig. 14 Deflections for low moment loading.

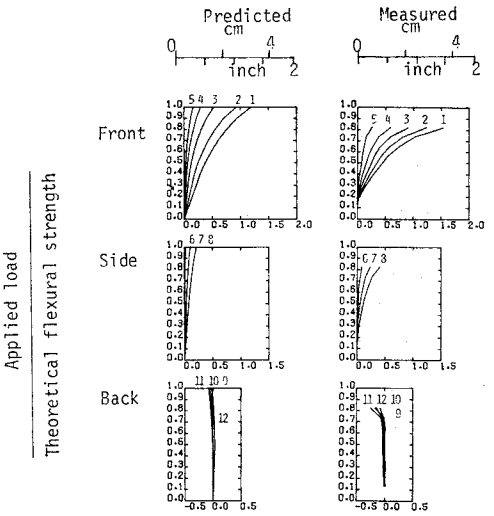

Fig. 15 Deflections for high moment loading.

lysis the slab was considered fixed at the column perimeter whereas the results indicated significant rigid body rotations at that section. Thus, good agreement between the absolute values for measured and computed deflections was not to be expected.

(4) Steel Strains.

Steel strains were measured at the selected locations shown in Fig. 16. Measured and calculated load-steel strain relationships are shown in Figs. 17 and 18. The calculated strains were deduced from the moment calculated as acting in the direction of the bar. It was assumed that the strain in that bar was caused by that moment alone and effects due to

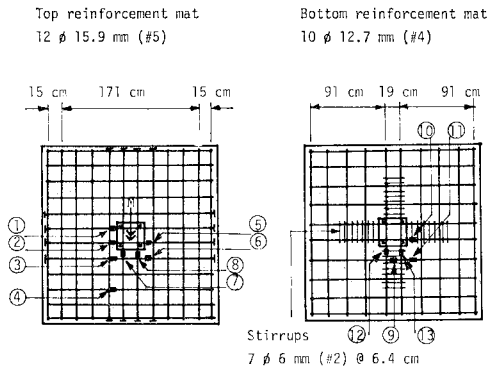

Fig. 16 Reinforcement and steel strain gages.

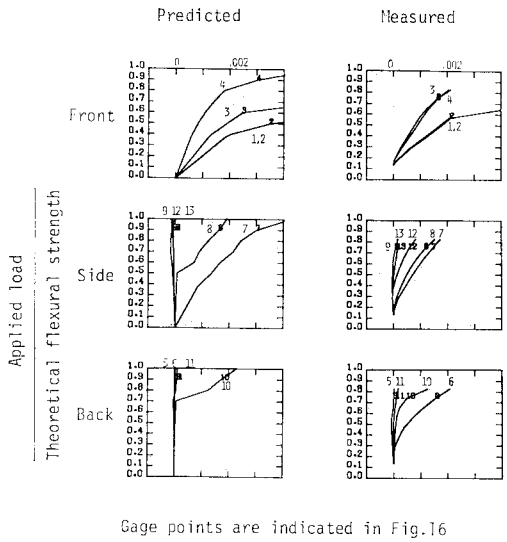

Fig. 17 Steel strains for high moment loading.

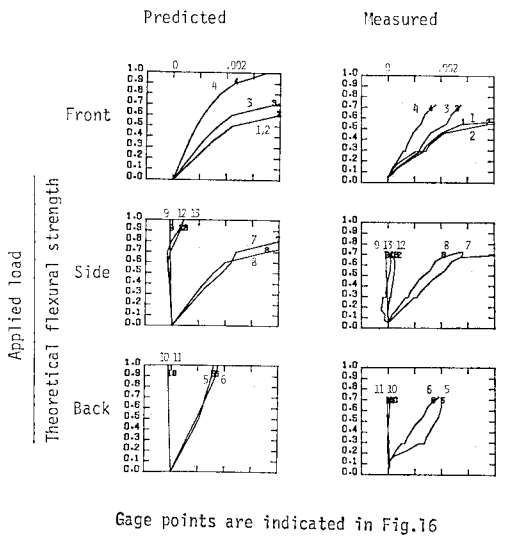

Fig. 18 Steel strains for low moment loading.

twisting moments and transverse shears were neglected. Strains were determined from the moments using the bending section properties of the slab.

The predicted and measured results in Figs. 17 and 18 show close similarities as to the distribution of steel strains around the column, the change in those strains with load and the sequence of progressive yielding. Those results appear to support the validity of the method of analysis for prediction of the stresses in the vicinity of the column in inelastic stage of behavior. From a comparison of experimental and theoretical findings for the change in strain in the bars with load, and in reference to the computed stresses presented by Figs. 6, 8, 9, 10 and 11, the following conclusions were developed concerning the effectiveness of the reinforcing bars in the immediate vicinity of the column.

a) Significance of Measured Strains for High Moment Loading.

Reference is made to Fig. 17. The behavior of top bars crossing the front face *AB* (Gages 1 and 2) is to be expected from high bending moment that must act at that location. Yielding of these bars at about 60 percent of the collapse load means that large rotations and large crack width must develop at the front face prior to collapse.

The behavior of the top bars crossing the side face *BC* (Gage 7 and 8) can also be related to the bending moment which analysis shows is largest for face *BC* adjacent to the front corner of the column. High twisting moments at the same location could have also increased the strain in the bar containg gage 7. The mechanism that caused tensile stresses to develop in the bottom bar (Gage 12) at the front corner at relatively early values of applied load is not obvious. According to the analysis very high shears act downwards in that area. Those shears are the result of combined shear force effects and torsion effects. Thus, inclined cracking within the slab is likely at this section earlier in the load history than normally assumed for connections not transferring moment. Therefore this bottom reinforcing bar is probably more essential as a shear transfer reinforcement restraining the vertical displacement of the slab than is the case for a connection not transferring moment.

The strain in the top bar just outside of the back corner of the column (Gage 6) might be expected to be small because calculated bending moment are small at that location. However, measurements showed markedly contradicting behavior and eventually yielding occurred at this location.

The portion of the slab to the side of the column is subjected to bending moment in the *Y* direction as apparent from Fig. 8 and twisting moments. The combination of those moments causes a principal

moment acting in a direction inclined at about 45 degree to the direction of the bar containing Gage 6. The analysis showed that this principal moment to be large enough to cause yielding of the bar for the length ranging from the front corner of the side face of the column to the middle of the side face of the column. Debonding probably causes the high tensile strain in the bar in that area being transmitted to the location of the gages.

From the analyses the yielding of the bottom bars crossing the back face *CD* is to be expected because of the high bending moments predicted for that location at failure. The probability of obtaining tensile strains at that location at relatively low loads is not obvious since the external loads create a static moment at that location opposite in direction to the moment indicated by the analysis.

The top bar and bottom bar crossing the side face *BC* and near the back corner show no appreciable strains. This point was close to center of rotational displacement for the slab. The analysis predicts small moments in the direction of this bar and the shear stress due to shear force are small in this area.

b) Significance of Measured Strains for Low Moment Loading.

The top bars passing through the column in the direction of the unbalanced moment are effective for resisting bending moments creating tensions at both the front face *AB* (Gage 1 and 2) and back face *CD* (Gage 5) of the column. The bottom bars in the same direction are not effective, even as compression reinforcement in resisting bending moments because in the typical thin building slab it is not possible to position those bars close enough to the compression surface of the slab to be effective.

The top bars passing through the column transverse to the direction of the unbalanced moment (Gage 7 and 8) are effective for resisting bending moments in that direction as well as resisting torsional moments created at the side faces by the unbalanced moments acting on the extension of the slab defined by lines passing through the front and back faces of the column. The bottom bars in the same direction (Gage 12 and 13) are effective for the portion of the side face of column. The stress in those bars is probably caused by high transverse shears together with torsions.

The top bars in the direction of the unbalanced moment and positioned immediately outside of faces of the column (Gage 3 and 6) are effective for resisting torsions acting at the side faces of the column. They are also effective in twisting the side portions of the slab sufficiently to transfer some of the unbalanced moment to the back face of the column once yielding occurs for the bars passing through the front of the column. Bottom bars in the direction of the unbalanced moment are ineffective in a low moment loading situation.

4. CONCLUSIONS

The following conclusions are drawn from this study.

(1) For distances as one slab thicness to the column face, finite element plate bending analyses can provide reasonable predictions of the likely shears, moments and torsions acting on finite areas of a connection transferring moment between the slab and column.

(2) An incremental linearization procedure that recognizes variations in stiffness and yielding with the direction of the reinforcement and the principal moments can be used to extend finite element plate bending analyses into the inelastic range.

(3) Capacities of connections should not be predicted by extrapolating forces determined from an elastic finite element analysis. An inelastic analysis such as that described in conclusion (2) is required.

(4) In the inelastic range there is considerable redistribution of moments and shears between the column faces as the stiffness of slab segment framing into each column face changes with loading. That redistribution can be predicted by the analysis described in conclusion (2).

(5) The analysis described in conclusion (2) correctly predicts the relative proportions for the deflections at various points adjacent to a connection. However, that procedure under-estimates actual deflections. To correctly predict actual deflections, that procedure will have to be modified to take account of the lesser stiffness of a slab for twisting moments and the bond slip of the reinforcing bars passing through the column.

(6) The ACI 318-77 procedure for determining shear stresses at a connection transferring moment provides a realistic measure of the shear stress on the front column face but under-estimates shear stresses on the side column face. The ACI procedure does not provide a realistic model for the manner in which moments and shears are transferred through a connection.

ACKNOWLEDGEMENTS

This paper was based on a Ph.D. thesis by the first author submitted to the University of Washington under the supervision of the second author. Experimental works were carried out at the Structural Research Laboratory of the Department of Civil Engineering of the same university. The research project was funded by the National Science Founda-

tion under grant GK-16373 and Reinforced Concrete Research Council under project No. 32.

Helpful comments and criticisms of Professor A.H. Mattock is gratefully acknowledged. Contributions were made to the execution of this series of investigation by Messrs. Anderegg, Mohaghe, Amin and Cooper, former graduate students, to all whom thanks are given.

APPENDIX. TEST PROGRAM

A.1 Test Specimens.

The specimens consisted of a 210 cm (7 foot) square slab supported on a central column as shown in Fig. 1. The column was 30 cm (12 inches) square, and the slab 15 cm (6 inches) thick. The column extended below the bottom of the slab a distance of 104 cm (41 inches), and horizontal loads were applied at a point 104 cm above the top of the slab. The slab was loaded at 60 cm (2 foot) intervals along a line lying 15 cm (6 inches) inside its perimeter. The specimens were intended to represent to approximately three quarter scale the portion of a flat slab frame extending from an interior column out to the region of contraflexure in the slab and between points of contraflexure in the column. Two loading patterns were used. For a high moment loading the ratio of the moment transferred to the column to the shear, M/V, was nominally 58 cm (23 in.). For a low moment loading the M/V ratio was nominally 13 cm (5 in.). The fraction of the loads applied at each loading point are shown in Fig. 1. Minor variations from those values occurred due to friction in the test set-up.

A.2 Materials and Fabrication.

High early strength cement, river sand and coarse aggregate of 19 mm (3/4 inch) in maximum size were used for all specimens. The coarse aggregate was a rounded river gravel with a bulk density of about 1 680 kg/m^3 (100 pounds per cubic foot). Approximately five batches of concrete were used to cast each specimen. At least two 15×30 cm (6×12 inch) cylinders were taken from each batch and used to determine the concrete compressive strength. The strength was determined by the average for the batches of concrete placed adjacent to and in the column connection. ASTM Grade 50 (equivalent to SD 35) deformed reinforcing bars for bars of size ϕ 9.5 mm (#3) and Grade 60 (equivalent to SD 40) for size ϕ 12.7 mm (#4) and greater were made from the same heat of steel. Plain ϕ 6 mm (#2) bars were used in some cases as stirrup reinforcement. The tensile properties of the reinforcing steel are as follows.

Table 2

Bar Size ϕmm	Yield Point (kg/cm^2) (ksi)	Tensile Strength (kg/cm^2) (ksi)
6 (#2)	4 310 (61.5)	5 590 (79.8)
9.5 (#3)	3 560 (50.9)	5 000 (71.4)
12.7 (#4)	4 830 (69.0)	7 600 (108.5)
15.9 (#5)	4 520 (64.5)	7 290 (104.5)

All specimens were reinforced with both tension and compression steel, and the bar sizes and spacing in each mat are indicated in Fig. 16. The compression steel ratio was equal to approximately half the tensile steel ratio. Care was taken to provide 19 mm (3/4 inch) of cover over the outside bars of the tension and compression mats in the slab. The layout of shear reinforcement in the form of rectangular stirrups with 135 degree end hooks are also shown in Fig. 16. Columns were reinforced with ϕ 22 mm (# 7) deformed bars continuous through the slab and placed in the corners of the column so that there was a concrete cover of 29 mm (1-1/8 inch) on each side of the bars. Rectangular ties for the columns were made from ϕ 9.5 mm (#3) deformed bars spaced at 11.4 cm (4-1/2 inch) centers along the length of the column. No column ties were placed in the slab to column junction.

A.3 Instrumentation.

Electrical resistance strain gages were used to measure strains at least 13 selected locations on the tension and compression reinforcing mats, and 7 locations on the compression surface of the slab. The locations for the steel strain gages are shown in Fig. 16. Deflections at 12 selected locations on the tension surface of the slab as indicated in Fig. 7 were measured by a precision level. Dial gages were also used to measure angular rotations at the slab-column connection. Load cells were used to measure the forces in one of the rods activated by each jack including the jack supplying the horizontal restraint at the top of the column. The output from those load cells was monitored continuously by a Sanborn automatic strain recorder.

A.4 Test Procedure.

Vertical loads were applied to the specimen by a series of hydraulic jacks. These jacks transmitted their loads to the slab through a system of articulated loading beams, steel rods and rocker supports. These jacks were connected to a common punping and indicating unit. To simulate the effects of axial loadings on the column and to provide initial stability to the test set-up, the column was prestressed to the laboratory floor by a rod passing through a duct located at the center of the column. The prestressing force in this rod was held at 22.5 ton (50 kips). For all specimens the overturning moments

caused by the loads applied to the slab were balanced by jacking horizontaly between the top of the column and an independent reaction frame. The applied loads were increased monotonically in equal increments until failure occurred or until the specimen deflected about 2.5 cm (1.0 inch). For loads causing deflections greater than 2.5 cm the load was increased in increments causing increase in deflection of about 0.8 cm (0.3 inch). The loads were chosen so that failure was usually reached in about 12 increments. After each load increments, a complete set of readings was taken on all gages. The crack patterns were recorded and measurements were made of the crack widths in the vicinity of the column. Some of the specimens deflected about 7.5 cm (3.0 inches) without failure occurring. At this deflection, continuing deformations could not be accomodated within the limits of the test set-up. Loading was therefore discontinued.

A.5 Test Results.

Crack patterns, deflections and steel strains for the two test specimens are reported in Section 3 of the main text. Concrete strengths and ultimate strengths are as follows.

Table 3

Specimen	Concrete Strength (kg/cm²) (psi)	Shear V (ton) (kips)	Moment M (t-cm) (k-in)
0.96 EL 0.33	289 (4 130)	26.8 (59.5)	386 (338)
0.96 EH 0.33	259 (3 700)	20.1 (44.7)	1 009 (883)

REFERENCES

1) ASCE-ACI Committee 426 : The Shear Strength of Reinforced Concrete Members-Slabs, Journal of the Structural Division, ASCE, Vol. 100, No. ST 8, pp. 1543～1591, August, 1974.
2) ACI Committee 318 : Building Code Requirements for Reinforced Concrete (ACI 318-77), American Concrete Institute, Detroit, Mich., 1977.
3) Hognestad, E. : Shearing Strength of Reinforced Concrete Column Footing, Journal of the American Concrete Institute, Vol. 50, No. 3, pp. 189～208, Nov., 1953.
4) Kinnunen, S. and H. Nylander : Punching of Concrete Slabs without Shear Reinforcement, Transactions No. 158, Royal Institute of Technology, Stockholm, Sweden, 1960.
5) Kinnunen, S. : Punching of Concrete Slabs with Two-Way Reinforcement with Special Reference to Dowel Effects and Deviation of Reinforcement from Polar Symmetry, Transactions No. 198, Royal Institute of Technology, Stockholm, Sweden, 1963.
6) Di Statio, J. and M.P. Van Buren : Transfer of Bending Moment between Flat Plate Floor and Column, Journal of the American Concrete Institute, Vol. 57, No. 3, pp. 299～314, Sept., 1960.
7) Moe, J. : Shearing Strength of Reinforced Concrete Slabs and Footings under Concentrated Loads, Development Bulletin D 47, Portland Cement Association, Skokie, Ill. Apr., 1961.
8) Hanson, N.W. and J.M. Hanson : Shear and Moment Transfer between Concrete Slabs and Columns, Journal of the Portland Cement Association Research and Development Laboratories, Vol. 10, No. 1, pp. 2～16, Jan., 1968.
9) Hawkins, N.M. and W.G. Corley : Transfer of Unbalanced Moment and Shear from Flat Plates to Columns, SP-30, Cracking, Deflection, and Ultimate Load of Concrete Slab Systems, American Concrete Institute, Detroit, Mich., pp. 147～176, 1971.
10) Lenschow, R.J. and M.A. Sozen : A Yield Criterion for Reinforced Concrete Slabs under Biaxial Moments and Forces, Civil Engineering Studies, Structural Research Series No. 311, University of Illinois, Urbana, Ill., July, 1966.
11) Cardenas, A. and M.A. Sozen : Strength and Behavior of Isotropically and Nonisotropically Reinforced Concrete Slabs Subjected to Combinations of Flexural and Torsional Moments, Civil Engineering Studies, Structural Research Series No. 336, University of Illinois, Urbana, Ill., May, 1968.
12) Clough, R.W. and C.A. Fellipa : A Refined Quadrilateral Element for Analysis of Plate Bending, Proceedings, Second Conference on Matrix Methods in Structural Mechanics, Wright-Patterson Air Force Base, Ohio, 1968.
13) Wilson, E.L. : SOLID SAP, A Static Analysis Program for Three Dimensional Solid Structures, University of California, Berkeley, Calif., Structural Engineering Laboratory Report, UC-SESM-71-19, 1971.

(Recived January 22, 1978)